

Frequency Domain Identification of Structural Dynamics Using the Pole/Residue Parametrization.

Etienne Balmès (DRET / AC)
ONERA, Structures Direction

ABSTRACT

The pole/residue parametrization has been traditionally used in single and multiple degree of freedom identification methods for structural dynamics. By considering residues as secondary unknowns that are solution of a least-squares problems, the non-linear optimization linked to this parametrization can be performed with the poles as only unknowns. An *ad hoc* optimization scheme, based on the use of gradient information and allowing simultaneous update of all poles, is proposed and shown to work in many situations. The iterative nature of the algorithm and the use of poles as only unknowns permits simple user interactions and generally allows the construction of models that contain all physical modes of the test bandwidth and no other modes. Models of structures generally verify many constraints (minimality, reciprocity, properness, positiveness) which are not necessarily verified by pole/residue models (which only assume linearity and diagonalizability). It is shown that constrained pole/residue models can be easily constructed as approximations of unconstrained pole/residue models and that this approach gives good representations of the initial data set. Difficulties, that a few years of experience with the proposed algorithms have shown to be typical, are highlighted using examples on experimental data sets.

1. INTRODUCTION

Identification methods can be classified using four main characteristics: the experimental data, the parametrization of the model, the cost function used to compare model and experiment, and the optimization algorithm.

For the test data, it is useful distinguish methods that use the measurements directly and methods that perform some form of non-parametric identification. By non-parametric identification, one means all methods that represent the properties of a linear system in the form of a function of discrete or continuous time (Markov parameters or impulse response) or frequency (transfer function). For non-linear systems higher order representation exist but are difficult to apply to complex structures.

Using the result of a non-parametric identification as “the experimental data set” presents the major advantage that effects of noise and external disturbances can be reduced at a relatively low cost [1] thus allowing the computationally intensive parametric identification to be performed on a relatively small and noise free data set. Most time and frequency domain identification methods use a data set that is the result of a non-parametric identification. The present study will be presented in the frequency domain where the quality of a model is generally evaluated.

Polynomial, state-space, second-order, rational fraction models are some of the parametrizations that have been considered for different identification methods. In most cases the only constraint taken into account is linearity. When identifying structures a number of other properties such as the reciprocity, diagonalizability, pole multiplicity, or the possibility to be represented by a second order model, are also desired

and/or assumed. Section 2 gives a review of assumptions related to structures and their implications in terms of properties of second order and pole residue models.

Parametric identification methods determine a parametric model that “optimally” matches the data. The definition of an optimum is based on the choice of a cost function that measures the difference between the data and the predictions of a parametric model. In the frequency domain, two costs have retained significant attention. The quadratic (LinLS) cost

$$J_{Quad} = \sum_{\text{sensor } j, \text{ actuator } k, \text{ frequency } l} |H_{jk}^1(\omega_l) - H_{jk}^2(\omega_l)|^2 \quad (1)$$

has nice mathematical properties (see section 3) and is the most widespread. The logarithmic (logLS) cost

$$J_{Log} = \sum_{\text{sensor } j, \text{ actuator } k, \text{ frequency } l} |\log(H_{jk}^1(\omega_l) / H_{jk}^2(\omega_l))|^2 \quad (2)$$

presents significant advantages for convergence and weighting of anti resonances but is computationally expensive [2].

The choice of a cost and parametrization is generally motivated by the algorithm used to determine the “optimal” model. One can generally distinguish synthesis methods which provide a direct transformation from data to model and tuning methods which improve an initial model. Tuning methods improve the results of a synthesis method and thus allow the correction of initial errors that always appear for real data. Section 3 presents, the IDRC method which tunes unconstrained pole/residue models using comparisons to measured FRFs and the IDRM method which tunes constrained pole residue models using comparisons with unconstrained models.

As for all identification methods limitations appear when applied to real data sets. The methods proposed in section 3 have now been used successfully for a few years and typical difficulties, that have been identified, are highlighted in section 4.

2. EXPECTED PROPERTIES FOR PARAMETRIC MODELS OF STRUCTURES

2.1. Linearity

Linear structures are generally represented by a model of the second order form

$$\begin{aligned} [Ms^2 + Cs + K] \{q\} &= [b] \{u(s)\} \\ \{y(s)\} &= [c] \{q\} \end{aligned} \quad (3)$$

In this model, the response is fully described by a finite number of *degrees of freedom* (DOFs) q that depend on time/frequency. The dynamic stiffness matrix $\mathcal{K} = Ms^2 + Cs + K$ gives the relation between the response of the model DOFs q and the model loads F_q . Symmetry of the dynamic stiffness corresponds to the assumption of reciprocity (see section 2.4).

Physical displacements (translations, rotations, stresses, strains, electric charge going through a piezoelectric, etc.) are called *outputs* y and assumed to be linearly related to the DOFs q through output shape matrices c ($y = c \{q\}$). For example, the matrix c associated with displacement outputs of a displacement based finite element corresponds to the evaluation of the element shape functions at the considered node.

Similarly loads (applied forces, pressure fields, control forces, gravity, tension on a piezoelectric, etc.) are represented by the product of time independent input shape matrices b and time/frequency dependent inputs u ($F_q(u) = bu$).

Models of the form (3) can also be written in the symmetric first order form

$$\begin{bmatrix} C & M \\ M & 0 \end{bmatrix} \begin{Bmatrix} \dot{q} \\ \ddot{q} \end{Bmatrix} + \begin{bmatrix} K & 0 \\ 0 & -M \end{bmatrix} \begin{Bmatrix} q \\ \dot{q} \end{Bmatrix} = \begin{bmatrix} b \\ 0 \end{bmatrix} \{u\} \quad (4)$$

$$\{y\} = \begin{bmatrix} c & 0 \end{bmatrix} \begin{Bmatrix} q \\ \dot{q} \end{Bmatrix}$$

The first order form (4) is associated to the left and right eigenvalue problems

$$\begin{bmatrix} C & M \\ M & 0 \end{bmatrix} \theta_R \Lambda + \begin{bmatrix} K & 0 \\ 0 & -M \end{bmatrix} \theta_R = 0 \text{ and } \Lambda \theta_L^T \begin{bmatrix} C & M \\ M & 0 \end{bmatrix} + \theta_L^T \begin{bmatrix} K & 0 \\ 0 & -M \end{bmatrix} = 0 \quad (5)$$

where Λ is the diagonal matrix of poles and the blocks of zeros in (4) imply that the eigenvectors θ can be decomposed into a displacement contribution ψ and a velocity contribution $\psi\Lambda$

$$[\theta_L]_{2N \times 2N} = \begin{bmatrix} [\psi_L]_{N \times 2N} \\ [\psi_L \Lambda]_{N \times 2N} \end{bmatrix} \text{ and } [\theta_R]_{2N \times 2N} = \begin{bmatrix} [\psi_R]_{N \times 2N} \\ [\psi_R \Lambda]_{N \times 2N} \end{bmatrix} \quad (6)$$

Note that the first order eigenvalue problems (5) are equivalent to the second order eigenvalue problems

$$[\lambda_j^2 M + \lambda_j C + K] \{\psi_{jR}\} = 0 \text{ and } \{\psi_{jL}^T\} [\lambda_j^2 M + \lambda_j C + K] = 0 \quad (7)$$

2.2. Diagonalizability

Except for the case of rigid body modes which will be addressed below, one can prove for proportionally damped structures and one assumes in other cases, that model (4) has a full set of $2N$ independent left ψ_{Lj} and right ψ_{Rj} modeshapes and $2N$ complex eigenvalues λ_j . The assumption that the model is diagonalizable is equivalent to writing the following orthogonality conditions for the $2N$ modes

$$\theta_L^T \begin{bmatrix} C & M \\ M & 0 \end{bmatrix} \theta_R = \psi_L^T C \psi_R + \Lambda \psi_L^T M \psi_R + \psi_L^T M \psi_R \Lambda = I_{2N} \quad (8)$$

$$\theta_L^T \begin{bmatrix} K & 0 \\ 0 & -M \end{bmatrix} \theta_R = \psi_L^T K \psi_R - \Lambda \psi_L^T M \psi_R \Lambda = -\Lambda$$

from these conditions, one easily transforms the model form (4) to the diagonal forms

$$\{\dot{\eta}\} = [\Lambda] \{\eta\} + \begin{bmatrix} 0 \\ \theta_L^T \begin{bmatrix} b \\ 0 \end{bmatrix} \end{bmatrix} u \text{ or } \{\dot{\eta}\} = [\Lambda] \{\eta\} + [\psi_L^T b] u \quad (9)$$

$$y = \begin{bmatrix} c & 0 \end{bmatrix} \theta_R \{\eta\} \text{ or } y = [c \psi_R] \{\eta\}$$

or the pole/residue form (also called rational fraction expansion)

$$\{y(s)\} = \sum_{j=1}^{2N} \frac{\{c \psi_j\} \{b^T \psi_j\}^T}{s - \lambda_j} \{u\} = \sum_{j=1}^{2N} \frac{[R_j]}{s - \lambda_j} \{u\} = [\alpha(s)] \{u(s)\} \quad (10)$$

In most cases, rigid body modes, which are not coupled to other modes by stiffness, are also not coupled by damping. As a result the model cannot be diagonalized. One has however a simple pole/residue form

$$[\alpha(s)] = \sum_{j=1}^{2N-2N_r} \frac{[R_j]}{s - \lambda_j} + \sum_{j=1}^{N_r} \frac{[T_{jR}]}{s^2} = \sum_{j=1}^{2N-2N_r} \frac{[R_j]}{s - \lambda_j} + \frac{[T_R]}{s^2} \quad (11)$$

The left and right eigenvectors and eigenvalues of real models come in complex conjugate pairs or are real. This leads to the pole/residue form

$$[\alpha(s)] = \sum_{j=1}^{N_c} \left(\frac{[R_j]}{s - \lambda_j} + \frac{[\overline{R}_j]}{s - \overline{\lambda}_j} \right) + \sum_{j=1}^{N_{\text{real}}} \frac{[T_j]}{s - \lambda_{j\text{Real}}} + \frac{[T_R]}{s^2} \quad (12)$$

2.3. Multiplicity

From (10), residue matrices linked to a single complex mode have the general form

$$[R_j]_{N_s \times N_A} = \{c \psi_j\}_{N_s \times 1} \{\psi_j^T b\}_{1 \times N_A} \quad (13)$$

which, as the product of a column vector $\{c \psi_j\}$ by a row vector $\{\psi_j^T b\}$, have obviously rank 1. Residue matrices with a higher rank correspond to multiple poles (more than one eigenvector linked to a single eigenvalue).

Although structures that have multiple poles are very unlikely (even axisymmetric structures often have enough dissymmetry in either their mass, damping, or stiffness properties to separate their theoretically double poles). The effective rank of a unconstrained residue matrix thus gives an indication of model accuracy (see section 3.3 and 4.3).

2.4. Reciprocity

Reciprocal models can be written in a symmetric form where the system matrices M, C, K are symmetric and input b and output c matrices of reciprocal (also called collocated) actuator/sensor pairs are the transpose of each other $b = c^T$. For models in such a form, the left and right complex modes are clearly equal and, for all collocated transfer functions, one has the scaling relation between the residue and the modal inputs and outputs

$$b_{\text{Col}}^T \psi_j = c_{\text{Col}} \psi_j = \sqrt{|R_j \text{Col}|} \quad (14)$$

2.5. Properness

Second order systems are proper in the sense that high frequency velocities tend to zero. Using the rational fraction form (10), one thus has for arbitrary b and c matrices

$$\lim_{s \rightarrow \infty} (s [\alpha(s)]) = \sum_{j=1}^{2N} \{c \psi_j\} \{b^T \psi_j\}^T = [c] [\psi \psi^T] [b] = 0 \quad (15)$$

which implies the properness condition on complex modes $\psi \psi^T = 0$. This condition can be used to provide transformations between the complex mode form (10) and the second order form (3), thus allowing the separate identification of mass, damping and stiffness properties [3].

2.6. Proportional damping

One often combines the contributions of complex conjugate poles in the following form

$$\left(\frac{[R_j]}{s - \lambda_j} + \frac{[\overline{R}_j]}{s - \overline{\lambda}_j} \right) = \frac{s(2\text{Re}(R_j)) - 2(\text{Re}(R_j)\text{Re}(\lambda_j)) - 2(\text{Im}(R_j)\text{Im}(\lambda_j))}{s^2 - 2\text{Re}(\lambda_j)s + |\lambda_j|^2} \quad (16)$$

where the hypothesis of proportional damping of a given mode corresponds to $\text{Re}(R_j) = 0$ [4,5].

2.7. Positiveness

An actuator/sensor pair is said to be collocated if the associated transfer function measures the power input to the structure. For passive structures the energy goes from the actuator to the structure which implies that the real part of a collocated force to velocity transfer function is always positive (this property has major implications for control applications [6])

Passive systems such as structures are positive for all inputs. Theoretically, it is possible to select a generalized input such that only one mode responds. As a result the contributions of all modes must be positive. In other words for all collocated FRFs

$$\operatorname{Re} \left(\frac{[R_j]s}{s - \lambda_j} + \frac{[\overline{R_j}]s}{s - \overline{\lambda_j}} \right) > 0 \quad \text{for all } j \text{ and } s = i\omega \quad (17)$$

which can be translated into conditions on the residues R_j . Although structures are known to be positive systems, actuator and sensor dynamics often lead to the measurement of transfer function that are not.

2.8. Truncation of high frequency modes

Structures are continuous systems so that they always have an infinite number of poles. To obtain a low frequency model of a structure one must thus retain the low frequency modes (in a model of the form (12)) and find an asymptotic representation of other modes

$$\begin{aligned} [\alpha(s)] = & \sum_{j=1}^{N_c} \left(\frac{[R_j]}{s - \lambda_j} + \frac{[\overline{R_j}]}{s - \overline{\lambda_j}} \right) + \sum_{j=1}^{N_{\text{Real}}} \frac{[T_j]}{s - \lambda_{j\text{Real}}} + \dots \\ & + \frac{[T_R]}{s^2} + [E_0 + E_1s + E_2s^2] \end{aligned} \quad (18)$$

For an arbitrary linear system the static contribution E_0 of truncated modes has no particular reason to be a sufficient representation of the asymptotic effect of truncated modes. For structures however, α represents the dynamic flexibility matrix so that the E_0 term corresponds to the residual static flexibility of truncated modes. Hundreds of studies related to Component Mode Synthesis methods have shown that for analytical models, the representation of the residual flexibility is generally necessary and sufficient to obtain a good representation of the low frequency dynamics. The use of higher order terms has been considered [7] but is generally not necessary.

Experience using the algorithms proposed in this paper has shown that the definition of residual terms is absolutely essential for a good identification and that the achievable accuracy is limited if these terms do not correspond to physical characteristics. Thus a test with a suspended structure should add a term in $1/s^2$ to account for the mass contributions to the dynamic compliance of suspension modes that are below the test bandwidth. Similarly, the use of a constant E term on a mobility measurement (force to acceleration) for which the residual stiffness takes the form Es^2 will limit significantly the quality of an identification.

2.9. Non-structural Dynamics

With the notable exceptions of structures with significant viscoelastic behavior [5] and measurement systems with significant time delays (Pade approximations of time delays contain real poles), possible real modes of structures are at very high frequencies so that their contributions can be assimilated to a constant asymptote. Dynamics linked to sensor or actuators are in series with the structure, they thus lead to poles with the number of sensors/actuators as multiplicity. The damping of such poles is generally quite different from the damping of structural poles so that it may be necessary to treat actuator/sensor identification and structural identification as two sequential problems.

3. IDENTIFICATION USING THE POLE/RESIDUE FORM

The methods described here and implemented in Ref. [8] decompose the identification problem in three steps, creation of an initial model, the identification of an ‘‘optimal’’ pole/residue model of the form (18) by tuning of the initial estimate, determination of an approximation of the identified model that verifies other desired properties (multiplicity, reciprocity, properness, positiveness, etc.)

3.1. Determination of an initial model

For the IDRC algorithm described in section 3.2, an initial estimate of the poles must be provided. Traditional single pole methods (circle fitting [9], narrowband single mode MIMO model [8], etc.) generally give very satisfactory results, but often leave out some modes (local modes or closely space modes) which can be added later. General identification algorithms can also be used to generate the initial pole but this leads to the necessity to eliminate computational poles. Although the author's preference is to build an initial pole set from single pole estimates, several criteria have been proposed to eliminate of computational poles and this approach is certainly worth considering (related issues are addressed in Refs. [10,2]).

3.2. Identification of a pole/residue model (IDRC algorithm)

The real objective of an identification is to identify all physical modes in the bandwidth and those only (no computational modes). Since such a result is never achieved by direct methods, some level of tuning is necessary. The method proposed here is to perform a non-linear optimization of the parameters of a pole/residue model of the form (18) with the LinLS cost (1) as a measure of error.

A number of authors have considered optimizing all the parameters of model (18) (poles λ_j and residues $\mathcal{R} = (R_j, T_j, T_R, E)$). However, for a very small test with 2 inputs, 5 outputs, and 5 identified modes there are already more than 120 parameters, and for 15 inputs and outputs and 30 modes the number jumps to 13785. Computational costs are thus critical even for moderately large models. To allow treatment of structural dynamics problem which typically have many FRFs and few poles, the IDRC algorithm (‘‘Identification De R esidus Complexes’’ first proposed in Ref. [11]) considers poles as unknowns and residues as implicit functions of the poles.

The response of a pole residue model of the form (18) clearly depends linearly on the residues and residual terms $\mathcal{R} = (R_j, T_j, T_R, E)$. One can thus rewrite the model (18) as a product of the form

$$\left[\alpha(\lambda_j, \mathcal{R}, s) \right] = \left[\Phi(\lambda_j, s) \right] \{ \mathcal{R} \} \quad (19)$$

From the decomposition (19) it appears that for a given set of poles λ_j the minimization of the cost (1) corresponds to the resolution of a linear least-squares problem in \mathcal{R} . In the IDRC algorithm, the residues \mathcal{R} associated to the unknowns (poles λ_j) are thus found by solving the linear least-squares problem

$$\{ \mathcal{R}(\lambda_j) \} = \arg \min_{\mathcal{R}} \left(\sum_{\text{sensor } j, \text{actuator } k, \text{frequency } l} |\Phi(\lambda_m, \omega_l) \mathcal{R}_{mjk} - \alpha_{jk}^{\text{Test}}(\omega_l)|^2 \right) \quad (20)$$

The numerical efficiency of least-square solvers makes (20) a very efficient way to find residues. Provided that the contributions of pairs of complex conjugate poles are grouped as shown in (18), the contributions of each pole is only important near its resonance. This leads to a very well conditioned least-square problem. (The case of extremely close poles has not been found to pose numerical problems). The number of columns in $\Phi(\lambda_j, s)$ (2 times the number of complex poles + the number of real poles + one column for rigid body modes + one column for the residual flexibility) is independent of the number of actuator/sensor pairs (measured FRFs) so that the solution is well suited for problems with many actuators/sensors.

The traditional explicit expression for the solution of a least-squares problem is

$$\{ \mathcal{R}(\lambda_j) \} = \left[\Phi(\lambda_j)^T \Phi(\lambda_j) \right]^{-1} \left[\Phi(\lambda_j)^T \right] \{ \alpha_{\text{Test}} \} \quad (21)$$

which leads to an explicit expression of the quadratic cost

$$J_{Quad}(\lambda_j) = \text{trace}\left((\alpha - \alpha_{Test})^T (\alpha - \alpha_{Test})\right) = \text{trace}\left(\alpha_{Test}^T (I - \Phi(\Phi^T \Phi)^{-1} \Phi^T) \alpha_{Test}\right) \quad (22)$$

From (22), the derivative of the quadratic cost J with respect to the parameter θ (here this parameter is the real or imaginary part of the different poles) can be computed explicitly [12]

$$\frac{\partial J}{\partial \theta} = 2(\alpha - \alpha_{Test})^T \frac{\partial \Phi}{\partial \theta} R \quad (23)$$

The principle of the IDRC algorithm is to optimize the unknowns (poles λ_j) while recomputing the residues at each step. The computation of residues is expensive so that good initial guesses and optimization procedures that improve results in a few steps are needed. As will be shown in section 4.2 the conditioning linked to the pole optimization is poor, so that, except for one pole models, traditional optimization algorithms have so far not given results at an acceptable cost.

Applications shown in this paper use an *ad-hoc* optimization procedure [8] which can be summarized as follows. The sign of the derivatives (23) is used to determine if the real and imaginary parts of the different poles are over- or underestimated. Assuming that the error made on other poles does not change the sign of the derivatives for a given pole, a step on the real and imaginary parts of all poles is done at each iteration. The step sizes associated to the real and imaginary parts of different poles are divided by two when the sign of the gradient changes.

This approach is not guaranteed to converge, but in practice it gives very good results in most cases at an acceptable computational cost (since all the poles are updated simultaneously the number of iterations needed rarely exceeds 50). Cases with non-converging poles often correspond to computational modes and can be otherwise corrected by resetting this particular pole after optimization of the other poles.

3.3. Constrained pole/residue models (the IDRM algorithm)

As shown in section 2, one usually expects a number of properties from a structural model. Pole/residue models of the form (18) assume that the system is linear and diagonalizable and that the residue flexibility E gives a sufficient representation of truncated high frequency modes.

Other constraints are very difficult to take into account in the IDRC approach which led to the development of the IDRM algorithm ("Identification de Résidus Multiples"). The objective of this algorithm is to find a model whose residue matrices are close to those of the identified model of the form (18) (i.e. such that the norm of their difference is small) but verify additional constraints of minimality, reciprocity, properness or proportional damping.

Minimality corresponds to the constraint on the rank of the residue matrix found for single poles (see section 2.3). By definition, the singular value decomposition of a matrix provides optimal (in the sense of the matrix norm) rank constrained approximations. Thus the best approximation of rank n_j of a matrix (for a residue matrix this corresponds to a pole of multiplicity n_j) is found by retaining the contributions of its first n_j singular values

$$\tilde{R}_j = \sum_{l=1}^{n_j} U_{jl} \sigma_{jl} V_{jl}^T \text{ with } R_j = U_j \Sigma_j V_j^T \quad (24)$$

with the error linked to using a minimal approximation of the non-minimal model (18) being given by the ratio of singular values $\sigma_{j,nj+1} / \sigma_{j,1}$.

For reciprocal models, the residue matrix must be symmetric. An approximation is thus found by taking the symmetric part of the identified matrix

$$\tilde{R}_j = (R_j + R_j^T) / 2 \quad (25)$$

and using a singular value decomposition (24) to simultaneously enforce minimality and reciprocity.

Approaches to enforce other conditions have also been considered but extend beyond the purpose of this paper (for the properness condition which allows the separation of mass, damping and stiffness properties see Ref. [3]).

4. APPLICATIONS TO EXPERIMENTAL DATA SETS

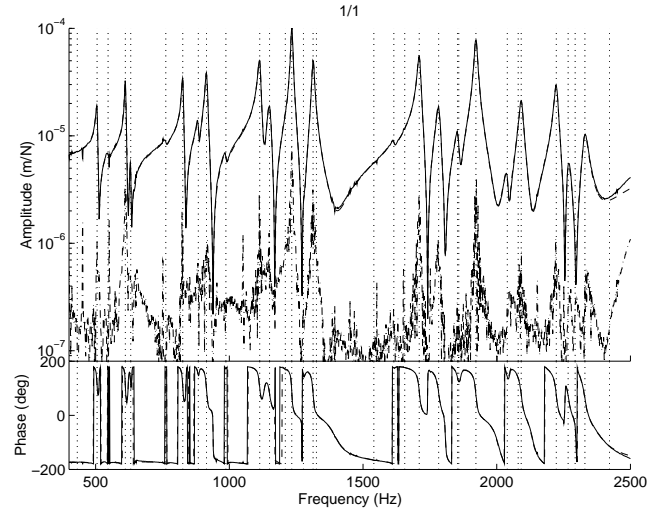


Fig. 1: Typical FRF/model comparison, 30 pole model with 225 FRFs. Data taken on the ONERA active plate experiment (EPA) [13]. (—) measured FRF α_{Test} , (---) model FRF α_{Model} , (-.-) $\alpha_{Test} - \alpha_{Model}$.

Experience has shown that the use on real data of the IDRC/IDRM identification procedure is fairly robust. A typical result is shown in figure 1 for a case with 32 poles, one of which is heavily damped. For this broadband model, both magnitude and phase of test and model overlay so well (the lines are barely distinguishable) that a better indication of model quality is given by the magnitude of the difference $\alpha_{Test} - \alpha_{Model}$ (more than 20 dB below the response in the figure).

The following sections will highlight typical limitations of the procedure since this will be more helpful for practical applications and extensions of the proposed methods than any number of good results.

4.1. Limitations of the residue estimation phase

The first use of the IDRC algorithm is the estimation of residues without update of the poles. The use of residual terms is a first requirement. For the EPA test, an heavily damped pole with its frequency outside the band is needed to account for the frequency dependent behavior of the piezoelectric patches uses as sensors/actuators. Such poles have a role similar to that of the residual flexibility and can be considered as residual terms.

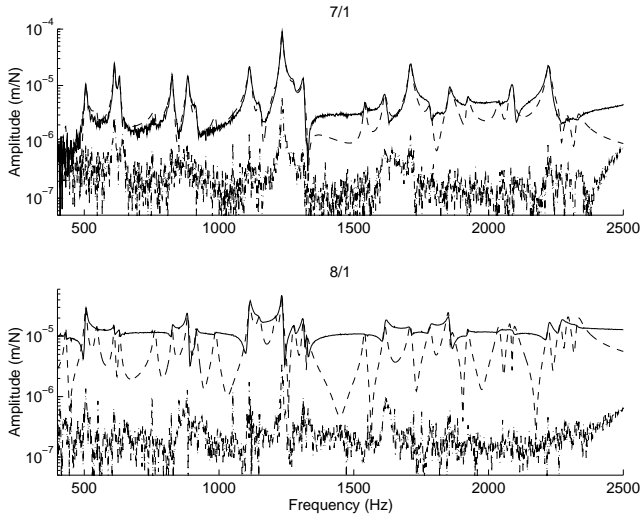


Fig. 2: Influence of residual terms in the EPA test. (—) α_{Test} measured FRF, (---) α_{Model} for model *without* residual terms, (-.-) $\alpha_{Test} - \alpha_{Model}$ for model *with* E asymptote and heavily damped pole.

For two FRFs, figure 2 shows the identified model without residual terms. It appears that only the low frequency range of FRF 7/1 is not so bad. FRF 8/1 is very typical of an FRF with high residual flexibility contribution. The error drops extremely rapidly (here the norm of $\alpha_{Test} - \alpha_{Model}$ is 40 dB below the response) as soon as such a contribution is added. In most test configuration and a good fraction of FRFs, residual stiffness and rigid body mode contributions (for suspended structures) are necessary and sufficient for a good fit.

The fact that appropriate residual terms are needed to obtain good results can have significant effects on the choice of the test bandwidth. Figure 3 shows such an example. The two modes above the selected band have a strong contribution so that the fit is poor and show peaks that are more apparent than needed (in the 900-1100 Hz range the FRF should look flat). This type of problem can become acute if the size of residues increase with frequency (piezoelectric patches can lead to such cases) and may require the use of wide frequency bands. Note also that similar errors in residue estimates are found if the pole of a dominant mode is not accurate enough.

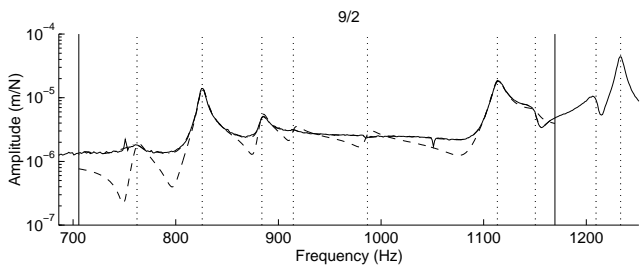


Fig. 3: Influence of error on a significant mode. (—) α_{Test} measured FRF, (---) α_{Model} for 7 poles in the band shown by vertical solid lines, (-.-) α_{Model} for model also considering two poles above the band.

A typical approach used to limit the effects of errors on large modes is the segmentation of the frequency band during the estimation. For a given segmentation of the frequency range, residues can be estimated using poles within the band and usual asymptotic contributions (18) (**type 1**) or all poles of the test bandwidth and retaining shapes associated to modes of the current band (**type 2**). Once local models determined, broadband

comparisons are only valid after a determination of broadband asymptotic contributions (since the local asymptotes cannot be combined into a single broadband model). For narrow band models of types 1 and 2, figure 4 shows the difference between the local and global model error. Two important facts appear in the figure. The segmentation approach does work even to recreate a global model. The use of a richer basis for residual terms (type 2 model) increases accuracy (for both local and global models).

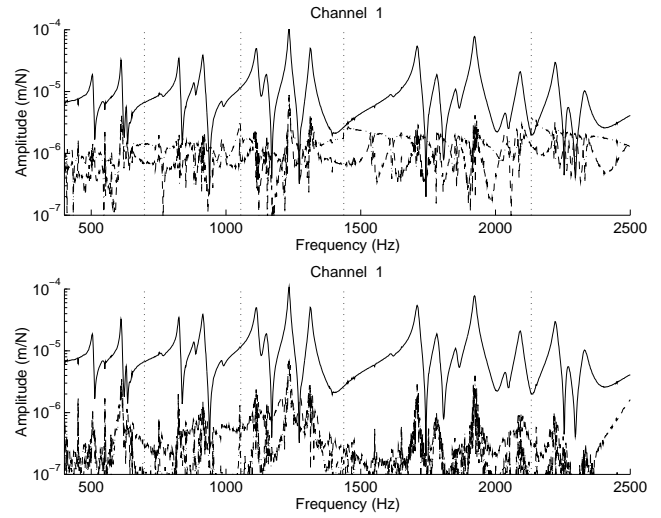


Fig. 4: Frequency band segmentation approach (frequency bands shown as vertical dashed lines) of type 1 (above) and 2 (below) : (—) measured FRF, (---) $\alpha_{Test} - \alpha_{Model}$ for local models, (-.-) $\alpha_{Test} - \alpha_{Model}$ for global model.

In many cases frequencies of estimated FRFs go down to zero. The first few points in these estimates generally show very large errors which can be attributed to both signal processing and limitations of sensors. Figure 5 shows a typical case where the first few points are in error by orders of magnitude. Of two models with the same poles, the one that keeps the low frequency erroneous points has a very large error while the other gives an extremely accurate fit of the data.

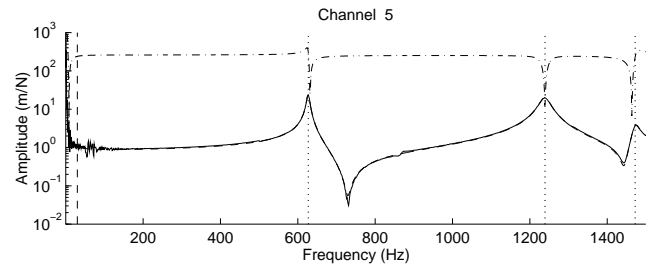


Fig. 5: Influence of erroneous low frequency points. (—) α_{Test} measured FRF, (---) $\alpha_{Test} - \alpha_{Model}$ for model down to 0 Hz, (-.-) $\alpha_{Test} - \alpha_{Model}$ for model >30 Hz (dashed line).

4.2. Convergence of the pole update phase

Application of the IDR algorithm is only valid if the identified unconstrained model is close to verifying the imposed constraints. This generally implies that the identified unconstrained model need to be very accurate. As a result optimization of the pole positions is almost always a necessity.

Ad-hoc algorithms such as the one proposed in section 3.2 are not guaranteed to converge (one can easily construct cases where they do not converge). The difficulty is however that algorithms with better mathematical foundations are associated to much higher computational costs which have so far limited their use.

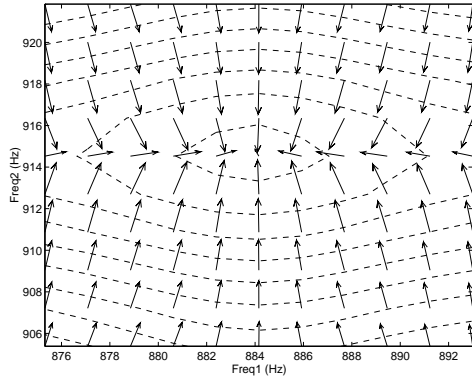


Fig. 6: Iso-cost lines (---) and gradient directions for the optimization of two pole frequencies.

A second limitation is the poor conditioning typically found for the optimization problem. Figure 6 shows the cost map and gradient directions for the optimization of two frequencies allowed to vary by 1%. The cost is much more sensitive to the first frequency so that the gradient gives a poor indication of the direction of the actual minimum. By only using the sign of the gradient and stepping on all poles simultaneously ad-hoc algorithm clearly converges well in this case. Better optimization algorithms are desirable and might alleviate the need to start with a good initial guess.

The level of accuracy needed for a given set of parameters is clearly a very important question which up to now as only been partially addressed. It appears rapidly in practice that the optimal set of poles significantly depends on the objective function used. This is illustrated in table 1, where poles that are “optimal” in different senses (different frequency bands) are compared. In this table and in other examples, typical variations are 0.05% for optimal frequencies and 10% for optimal damping ratio. Such errors do however significantly degrade a fit so that optimums need to be known with much better accuracy. The variations in the optimums can be related to errors in residual terms, but as seen in section 4.2 the choice of residual terms is a very difficult problem.

Table 1: Variations in the “optimal” set of poles. Case 1: local estimates based on 15 frequency points. Case 2: identification with five modes of the considered band. Case 3: 2 modes above and 2 below the frequency band are considered.

	Nominal	Case 1	Case 2	Case 3
$\Delta\omega$ (%)	762.1	0.0	0.039	0.020
	825.6	0.0	0.025	0.022
	884.2	0.0	-0.025	-0.024
	914.5	0.0	0.012	0.005
	986.1	0.0	0.073	0.076
$\Delta\zeta$ (%)	0.657	0.0	42.5	13.7
	0.401	0.0	0.0	-1.6
	0.484	0.0	15.7	-2.2
	0.474	0.0	6.7	4.0
	0.533	0.0	68.4	14.4

Finally, it should be noted that the IDRC method aims at constructing a single broadband MIMO model which implies that poles are common to all FRFs. Changing actuators/sensors for different tests, doing sequential SIMO tests on a non-linear structure, having insufficient frequency resolution are possible reasons that may lead to data sets that do not comply with this hypothesis. It may thus be impossible to obtain a single pole set that will give a correct estimation for all FRFs (see example in Ref. [12]).

4.3. Applications of the IDRM algorithm

The IDRM algorithm finds constrained approximations (minimal, reciprocal, proper, positive, etc.) of the unconstrained pole/residue model resulting from the use of IDRC. In most practical cases, minimality is the most difficult constraint so that it will be the only one illustrated here (note that minimality can only be considered for MIMO tests).

For the identified EPA model shown in figure 1, a minimal realization (poles with multiplicity 1) was computed. The ratios σ_2/σ_1 of singular values σ_3/σ_1 are shown in figure 7. For a few modes these ratios are above 0.1. For these modes however, the residues (shown by σ_j) are relatively small and there are other modes close in frequency (see the steep slopes of the high peaks). This highlights the fact that high singular value ratio are generally due to bad identification and/or close modal spacing (close modal spacing implies that it is quite difficult to separate the influence of two poles, see the example below). Ratios significantly above 0.1 generally mean bad identification and exceptionally multiple poles which are well indicated by the Multivariate Mode Indicator Function [14] (see the example below).

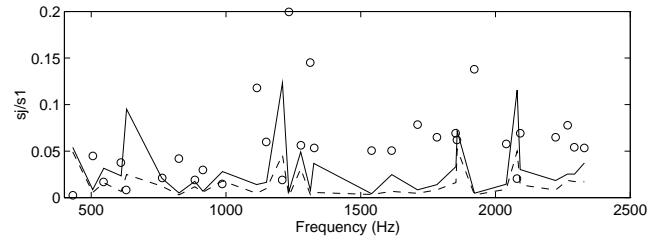


Fig. 7: Ratio (—) σ_2/σ_1 and (---) σ_3/σ_1 for decomposition of non-minimal model of the EPA test. Size of residues, given by σ_j , are shown by (o).

For good identifications, the use of a minimal model induces very small perturbations. For the EPA model with 3 inputs and 15 outputs, the LinLS error (1) increases from $1.1e-8$ to $1.4e-8$ and the logLS error (2) from 66.2 to 84.7. Such changes are barely discernible in figures such as figure 1 and are thus not shown here.

When creating a minimal model, residual terms are still essential but the rank constraint is not applicable (the static contributions of different high frequency poles are independent). When heavily damped or real poles are added to take into account actuator or sensor dynamics, these dynamics are applied to all inputs/outputs so that no rank constraint should be applied. For the EPA identification, an heavily damped pole is used at $\omega = 5900$ Hz, $\zeta = 0.9$. If a rank 1 approximation is used for this mode, the logLS error (2) jumps from 66.2 to 5094.8.

Figure 7 showed the fact that very close modes often lead to identified residue matrices with stronger non-minimal contributions. This fundamental difficulty linked to the transfer of contribution between close modes can be illustrated as follows. Figure 8 shows the Multivariate Mode Indicator Function for the EPA. The fact that two indicator functions have a minima near 1850 Hz indicates the presence of a double pole. These two poles are so close that one might consider that they are identical.

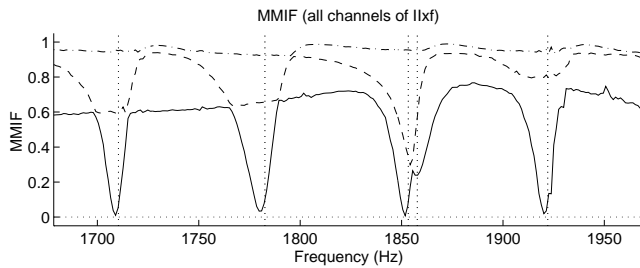


Fig. 8: Multivariate Mode Indicator Function [14] for 3-inputs and 15 outputs of the EPA. Note the 2 very close modes near 1850 Hz.

Table 2: Transfer of contributions of closely spaced poles. Global model with 1 or 2 poles near 1850 Hz.

ω (Hz)	ζ %	LinLS	LogLS	σ_2/σ_1	σ_3/σ_1
1853.3	0.306	1.97e-8	1.22e+2	0.47	0.01
1853.3	0.306	1.07e-8	0.83e+2	0.03	0.01
1857.8	0.542			0.07	0.05

Table 2 summarizes the results of a global fit obtained using 1 or 2 poles. The LinLS (1) and logLS (2) errors indicate that the error induced by retaining 1 mode instead of 2 is minor. Furthermore when using 1 mode, the singular value ratio clearly indicate a multiplicity of 2 which is expected. When using 2 modes, the quality of the identification of the second mode is not clearly minimal ($\sigma_2/\sigma_1 = 0.07$) but this error is almost certainly related to an identification error (non-optimal value for the second pole).

5. CONCLUSION

The proposed methods have demonstrated the possibility to use tuning approaches to create models that verify all constraints of interest for structures (linearity, diagonalizability, multiplicity, reciprocity, positiveness, properness, proportional damping) and yet contain all physical modes of the test bandwidth and those only.

The iterative nature of the IDRC algorithm and the use of poles as only unknowns leads to a user friendly and extremely efficient algorithm. Improved optimization strategies may lead to larger convergence regions. This should improve overall speed but user involvement will remain both desirable and necessary. Issues linked to residual terms and local/global frequency band selections need to be further addressed.

Although effectiveness has been demonstrated for a number of fairly complex cases, it is not always be possible to identify an unconstrained pole/residue model or to achieve sufficient accuracy to perform the step from unconstrained to constrained pole/residue model. Outside limitations of the optimization algorithms, there are fundamental reasons that lead to experimental data sets that cannot be accurately fitted by a parametric model. For the unconstrained pole/residue model, the two main reasons are non-linearity and time variance (modification of the system when performing sequential SIMO tests for example). For constrained models a number of problems may occur: actuator/sensor dynamics lead to non-minimal poles, force and displacement measurements that are not truly collocated lead to a non-reciprocal test, viscoelastic behavior with heavily damped poles lead to coupling of normal modes over a large band which is not compatible with the use of a proper model, etc.

6. ACKNOWLEDGMENTS

Many thanks to Gary Blackwood of MIT (now at JPL) and Benoit Petitjean of ONERA for providing many challenging data sets including those used as illustrations for this paper.

7. REFERENCES

- [1] Ljung, L., "System Identification: Theory for the User," Prentice-Hall, 1987
- [2] Jacques, R.N., *On-line System Identification and Control Design for Flexible Structures*, MIT Ph.D. Thesis, 1994, SERC report #11-94
- [3] Balmès, E., "New results on the identification of normal modes from experimental complex modes," *IMAC*, 1994
- [4] Liang, Z., Tong, M., Lee, G.C., "Complex Modes in Damped Linear Dynamic Systems," *Int. J. Anal. and Exp. Modal Analysis*, 1992, 7-1, pp. 1-20
- [5] Balmès, E., "Erreurs liées à la représentation de l'amortissement dans les modèles de systèmes complexes," *La Recherche Aéronautique*, 1996-1
- [6] Anderson, B.D.O., "A System Theory Criterion for Positive Real Matrices," *J. SIAM Control*, 1967, 5-2, pp. 171-181
- [7] Rubin, S., "Improved Component-Mode Representation for Structural Dynamic Analysis," *AIAA Journal*, 1975, 13-8
- [8] Balmès, E., *Structural Modeling Toolbox Version 2.0* (A toolbox for MATLAB™, Scientific Software Group (France), e-mail: info@ssg.fr)
- [9] Ewins, D.J., *Modal Testing: Theory and Practice*, John Wiley and Sons, Inc., New York, NY, 1984
- [10] Peterson, L., "Identification of Structural Dynamic Models from Closed-Loop Experiments," *AIAA/ASME Adaptive Structures Forum*, 1994
- [11] Balmès, E., "Integration of Existing Methods and User Knowledge in a MIMO identification algorithm for structures with high modal densities," *IMAC*, 1993, pp. 613-619
- [12] Balmès, E., *Experimental/Analytical Predictive Models of Damped Structural Dynamics*, MIT PhD Thesis, SERC Report # 7-93, 1993
- [13] Petitjean, B., Legrain, I., "Feedback controllers for broadband active noise reduction," *2nd European Conference on Smart Structures and Materials*, Glasgow, October, 1994
- [14] Williams, R., Crowley, J., Vold, H., "The Multivariate Mode Indicator Function in Modal Analysis," *IMAC*, 1985